Ouwens DM, de Ruiter ND, van der Zon GCM, Carter AP, Schouten J, van der Burgt C, Kooistra K, Bos JL, Maassen JA, van Dam H (2000) Growth factors can activate ATF2 via a two-step mechanism: phosphorylation of Thr71 through the Ras–MEK–ERK pathway and of Thr69 through RalGDS–Src–p38. *EMBO J* **21:** 3782–3793

Prmkhaokham A, Shimada Y, Fukuda Y, Kurihara N, Imoto I, Yang Z-Q, Imamura M, Nakamura Y, Amagasa T, Inazawa J (2000) Nonrandom chromosomal imbalances in esophageal sequamous cell carcinoma cell lines: possible involvement of the ATF3 and CENPE gene in the 1q32 amplicon. *Jpn J Cancer Res* **91:** 1126–1133

Perez S, Vial E, van Dam H, Castellazzi M (2001) Transcription factor ATF3 partially transforms chick embryo fibroblasts by promoting growth factor-independent proliferation. *Oncogene* **20:** 1135–1141

Sakamoto D, Prendergast GC (1999) New Myc-interacting proteins: a second Myc network emerges. *Oncogene* **18:** 2942–2954

Schorl C, Sedivy JM (2003) Loss of protooncogene c-Myc function impedes G1 phase progression both before and after the restriction point. *Mol Biol Cell* **14:** 823–835

Sears R, Leone G., DeGregori J, Nevins JR (1999) Ras enhances Myc stability. *Mol Cell* **3:** 169–179

Sears R, Nuckolls F, Haura E, Taya Y, Tamai K, Nevins JR (2000) Multiple Ras-dependent phosphorylation pathways regulate Myc protein stability. *Genes Dev* **14:** 2501–2514

Shachaf CM, Kopelman AM, Arvanitis C, Karlsson A, Beer S, Mandl S, Bachmann MH, Borowsky AD, Ruebner B, Cardiff RD, Yang Q, Bishop JM, Contag CH, Felsher DW (2004) MYC inactivation uncovers pluripotent differentiation and tumour dormancy in hepatocellular cancer. *Nature* **431:** 1112–1117

Shrivastava A, Yu J, Artandi S, Calame K (1996) YY1 and c-Myc associate *in vivo* in a manner that depends on c-Myc levels. *Proc Natl Acad Sci USA* **93:** 10638–10641

Tamamori-Adachi M, Hayashida K, Nobori K, Omizu C, Yamada K, Sakamoto N, Kamura T, Fukuda K, Ogawa S, Nakayama KI, Kitajiam S (2004) Down-regulation of p27 promotes cell proliferation of rat neonatal cardiomyocytes induced by nuclear expression of cyclin D1 and CDK4. *J Biol Chem* **279:** 50429–50436

Trumpp A, Refaeli Y, Oskarsson T, Gasser S, Murphy M, Martin GR, Bishop JM (2001) c-Myc regulates mammalian body size by controlling cell number but not cell size. *Nature* **414:** 768–773

Yin T, Sandhu G, Wolfgang CD, Burrier A, Webb RL, Rigel DF, Hai T, Whelan J (1997) Tissue-specific pattern of stress kinase activation in ischemic/reperfused heart and kidney. *J Biol Chem* **272:** 19943–19950

Zhang C, Gao C, Kawauchi J, Hashimoto Y, Tsuchida N, Kitajima S (2002) Transcriptional activation of the human stress-inducible transcriptional repressor ATF3 gene promoter by p53. *Biochem Biophys Res Commun* **297:** 1302–1310

Rheumatology 2005;44:332–336 doi:10.1093/rheumatology/keh505
Advance Access publication 14 December 2004

Effects of different corticosteroids on the development of osteonecrosis in rabbits

K. Miyanishi[1], T. Yamamoto[1], T. Irisa[1], G. Motomura[1], S. Jingushi[1], K. Sueishi[2] and Y. Iwamoto[1]

Objectives. **Osteonecrosis (ON) of the femoral head is a devastating complication occurring in patients receiving corticosteroid treatment. This study examined the effect of three corticosteroids on the development of ON in rabbits.**

Methods. **Thirty-nine rabbits were injected once intramuscularly with either 25 mg/kg prednisolone sodium succinate (PSL; 13 rabbits), 20 mg/kg methylprednisolone acetate (MPSL; 13 rabbits) or 20 mg/kg triamcinolone acetonide (TR; 13 rabbits). Four weeks after corticosteroid injection, the bilateral femora and humeri were examined histopathologically for the presence of ON. Haematological examinations were performed before and after corticosteroid injection.**

Results. **MPSL treatment (17/26 proximal femora, 65%) significantly increased ON incidence in the proximal femora compared with the levels seen after TR (4/26, 15%) or PSL (3/26, 12%) treatment ($P < 0.01$). Although not significantly increased in comparison with rabbits receiving PSL treatment (1/26 proximal humeri, 4%), ON incidence within the proximal humeri was significantly increased in MPSL-treated rabbits (6/26, 23%) in comparison with those seen in rabbits receiving TR (0/26, 0%) treatment ($P < 0.05$). Serum levels of cholesterol, triglyceride and free fatty acid were significantly higher 1, 2 and 4 weeks after corticosteroid treatment in rabbits treated with MPSL relative to rabbits receiving TR and rabbits with PSL treatment ($P < 0.05$).**

Conclusions. **MPSL treatment significantly increased ON incidence in rabbits over levels seen after TR or PSL treatment.**

KEY WORDS: Osteonecrosis, Corticosteroid, Rabbit, Hip.

Osteonecrosis (ON) of the femoral head is a serious complication of corticosteroid treatment [1, 2]. ON is typically observed in patients aged 30–60 and progresses to secondary osteoarthritis following subchondral collapse [1, 2]. A magnetic resonance imaging analysis demonstrated ON incidence of 44% for patients with systemic lupus erythematosus (SLE) [3]. Corticosteroid dosage has been found to be associated with the incidence of ON in SLE patients [4].

Prednisolone (PSL), methylprednisolone (MPSL) and triamcinolone (TR) are intermediate-acting corticosteroids widely used for treatment of various rheumatic diseases [5, 6]. Oral PSL at low doses is used to treat symptoms of mild to moderate SLE, while higher doses (1–1.5 mg/kg body weight) improve the survival of SLE patients [6, 7]. As PSL is poorly water-soluble, the addition of methyl groups produces MPSL, which can be used intravenously. Intravenous pulses of MPSL allow high doses of corticosteroids to be rapidly delivered to patients who cannot take oral medication and exhibit the severe manifestations of SLE [6]. In rabbits, a single injection of high-dose MPSL (20 mg/kg) results in ON lesions of the femur and humerus [8]. A fluorinated steroid, TR, is used to treat respiratory inflammation, rheumatoid arthritis and a variety of other inflammatory conditions [9].

To date, the effect of these different types of corticosteroids on ON development has not been well elucidated. Clinically, such attempts are often confounded by associated underlying diseases and differing administration methods (oral or intravenous). To address this question, this study was designed to investigate the effects of PSL, MPSL and TR on ON development in rabbits.

Materials and methods

A rabbit model of corticosteroid-induced ON was used in this study [8]. Administration of a single high dose (20 mg/kg) of MPSL, simulating a dose of human steroid pulse therapy, was used to cause ON lesions reproducibly in this model [8]. All experiments, after review by the Common Ethics Committee for Animal Experiments at Kyushu University, were conducted in accordance with the Guidelines for Animal Experiments of Kyushu University, Law no. 105, and the notification (no. 6) by the government and the Committee on Ethics in Japan.

Animals

Adult (defined as having the growth plate already closed) male Japanese white rabbits (Kyudo, Tosu, Japan), weighing 3.0–4.0 kg, were housed at the Animal Center of Kyushu University and maintained on a standard laboratory diet and water. Rabbits ranged in age from 28 to 32 weeks.

Treatment

Thirty-nine rabbits were injected once intramuscularly with 25 mg/kg body weight PSL sodium succinate (Shionogi, Osaka, Japan; 13 rabbits), 20 mg/kg body weight MPSL acetate (Upjohn, Tokyo, Japan; 13 rabbits) or 20 mg/kg body weight TR acetonide (Bristol-Myers Squibb, Tokyo, Japan; 13 rabbits) into the right gluteus medius. The corticosteroid doses used here were

[1]Department of Orthopaedic Surgery, Graduate School of Medical Sciences, Kyushu University, Fukuoka, Japan.
[2]Division of Pathophysiological and Experimental Pathology, Department of Pathology, Graduate School of Medical Sciences, Kyushu University, Fukuoka, Japan.

Submitted 27 August 2004; revised version accepted 2 November 2004.

Correspondence to: T. Yamamoto, Department of Orthopaedic Surgery, Graduate School of Medical Sciences, Kyushu University, 3-1-1 Maidashi, Higashi-ku, Fukuoka 812-8582, Japan. E-mail: yamataku@ortho.med.kyushu-u.ac.jp

determined to give equal glucocorticoid activities for each administration based on previously reported relative potencies (PSL:MPSL:TR = 4:5:5) [5]. Intramuscular injection of physiological saline was previously shown to produce no ON lesions in rabbits [8] and was not performed in this study.

Tissue preparation

Four weeks after corticosteroid injection, animals were anaesthetized by intravenous injection of pentobarbital sodium (25 mg/kg body weight; Abbott, Chicago, IL, USA), then killed by exsanguination via aortectomy. For examination by light microscopy, both femora and humeri (a total of four bone samples per rabbit) were obtained at the time of death and fixed for 1 week in 10% formalin, 0.1 M phosphate buffer (pH 7.4). Bone samples were decalcified with 25% formic acid for 3 days, then neutralized with 0.35 M sodium sulphate for 3 days. Samples were sectioned along the coronal plane for the proximal one-third and cut along the axial plane in the distal part (condyle). Lastly, specimens were embedded in paraffin, cut into 4-μm sections, and stained with haematoxylin and eosin.

Evaluation of ON

The entirety of the proximal one-third and distal condyles of both femora and humeri (a total of eight regions) were examined histopathologically for the presence of ON. A diagnosis of ON was made in blinded fashion by three of the authors (K.M., T.Y., T.I.), based on the diffuse presence of empty lacunae or pyknotic nuclei of osteocytes within the bone trabeculae, accompanied by surrounding bone marrow cell necrosis on the basis of published criteria for rabbit ON [8, 10]. A proximal or distal part of a bone is considered necrotic if it contains an ON lesion.

Haematological examination

Blood samples were obtained from fasting rabbits prior to experimentation (time 0) and 48 h and 1, 2, 3 and 4 weeks after corticosteroid injection. We examined the blood levels of cholesterol, triglycerides, free fatty acid and platelets.

Statistical analysis

Numbers of proximal or distal parts of femora and humeri with ON lesions were compared using the χ^2 test with Bonferroni methods for multiple comparisons. Haematological data obtained at each time point were compared using Bonferroni tests. Statistical analyses were performed using StatView J-5.0 software (SAS Institute, Cary, NC, USA). P values <0.05 were considered to be significant.

Results

Macroscopic and histopathological features

Macroscopically, regions exhibiting ON appeared as yellowish-coloured areas within the bone. Histologically, ON lesions exhibited an accumulation of bone marrow cell debris and the appearance of bone trabeculae with empty lacunae (Fig. 1). These findings were consistent for all osteonecrotic tissues. Little

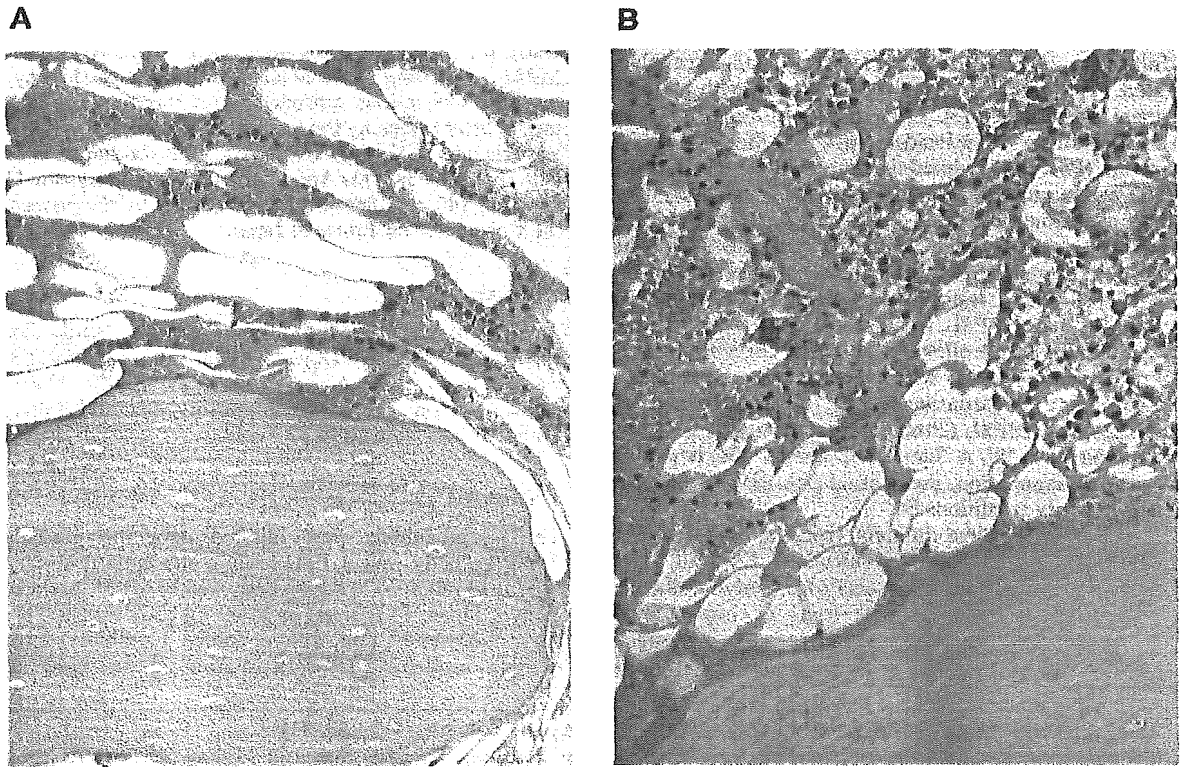

FIG. 1. Histological features of osteonecrosis in rabbits. Bone trabeculae demonstrate empty lacunae. The surrounding bone marrow tissue contains necrotic bone marrow cell debris. Little reparative tissues are observed in rabbits receiving MPSL treatment (A), while the osteonecrotic lesions are accompanied by adjacent reparative processes, including aggregation of macrophages and fibrous tissue invasion in rabbits treated with PSL (B). Haematoxylin and eosin, original magnification ×200.

TABLE 1. Prevalence and location of osteonecrosis of the femur in rabbits

Steroid	Number of femora	Number of femora with osteonecrosis: Proximal	Distal
PSL	26	3 (12%)	3 (12%)
MPSL	26	17 (65%)*	8 (31%)
TR	26	4 (15%)	2 (8%)

*$P < 0.01$ *vs* PSL and TR.

TABLE 2. Prevalence and location of osteonecrosis of the humerus in rabbits

Steroid	Number of humeri	Number of humeri with osteonecrosis: Proximal	Distal
PSL	26	1 (4%)	0 (0%)
MPSL	26	6 (23%)*	0 (0%)
TR	26	0 (0%)	0 (0%)

*$P < 0.05$ *vs* TR.

reparative response was observed in rabbits receiving MPSL treatment (Fig. 1A). However, in rabbits with PSL or TR treatment, the osteonecrotic lesions were accompanied by adjacent reparative processes, including aggregation of macrophages and fibrous tissues invasion (Fig. 1B).

Prevalence and location of ON

Prevalence and location of ON are shown in Tables 1 and 2. MPSL treatment significantly increased ON incidence in the proximal femur over the levels observed for TR or PSL treatment (Table 1) ($P < 0.01$). No significant differences, however, were observed in ON incidence of the proximal femur in rabbits treated with PSL and TR. Incidence of ON in the distal femur was not significantly different among the treatment groups (Table 1).

While the number of proximal humeri with ON lesions in PSL-treated rabbits did not change significantly when compared with rabbits receiving MPSL or TR treatment, the number of necrotic proximal humeri significantly increased in rabbits receiving MPSL in comparison with rabbits receiving TR treatment (Table 2) ($P < 0.05$). No ON lesions were observed in the distal humeri in any of the treatment groups (Table 2).

Haematological examination

Serum cholesterol levels were significantly higher in rabbits treated with MPSL than in rabbits with PSL treatment ($P < 0.01$ at 1 and 2 weeks; $P < 0.05$ at 3 weeks) and rabbits receiving TR ($P < 0.01$ at 1, 2 and 3 weeks; $P < 0.05$ at 4 weeks) (Fig. 2A). Serum levels of triglyceride were significantly higher in rabbits treated with MPSL than in rabbits with PSL treatment ($P < 0.01$ at 1, 2 and 4 weeks) and rabbits receiving TR ($P < 0.01$ at 1 and 2 weeks; $P < 0.05$ at 4 weeks) (Fig. 2B). Significantly higher levels of free fatty acid were observed in MPSL-treated rabbits than in rabbits treated with PSL ($P < 0.01$ at 1, 2 and 4 weeks; $P < 0.05$ at 3 weeks) and rabbits receiving TR treatment ($P < 0.01$ at 1, 2, 3 and 4 weeks) (Fig. 2C). There was no significant difference in serum levels of cholesterol, triglyceride and free fatty acid between rabbits receiving PSL and TR treatment at any time point tested.

Platelet numbers were decreased from pretreatment levels 1 week after corticosteroid injection in all treatment groups. The platelet levels were significantly higher in rabbits receiving PSL treatment than in rabbits with MPSL treatment and rabbits receiving TR at 1 ($P < 0.05$) and 2 ($P < 0.01$) weeks following corticosteroid treatment. At 3 and 4 weeks, levels of platelets were significantly lower in rabbits treated with MPSL in comparison with rabbits with PSL treatment and rabbits receiving TR ($P < 0.01$) (Fig. 2D).

Discussion

In this study, we adjusted three variables—glucocorticoid activity, biological half-life and administration method—to exclude potential experimental biases. Glucocorticoid activity generally includes anti-inflammatory, anti-allergic and immunosuppressive effects [5]. Corticosteroid doses were determined to result in each administration producing equal glucocorticoid activities, based on their reported relative potencies (PSL:MPSL:TR = 4:5:5) [5]. In addition, PSL, MPSL and TR are all intermediate-acting corticosteroids with similar biological half-lives (12–36 h) [11]. These drugs were injected intramuscularly according to the original rabbit ON model [8].

To date, there have been no reports comparing the incidence of human ON according to the different corticosteroid compounds used. Intra-articular TR hexacetonide for juvenile rheumatoid coxitis did not increase the risk of ON [12]. There is a case report in which depot corticosteroid injections for hay fever that included TR and MPSL caused ON [13]. However, to our knowledge, there seem to be no or few adult ON cases which have proved to be caused by systemic administration of TR alone. This is consistent with the low ON incidence in rabbits treated with TR in our study. Although the results showed a lower incidence of ON in rabbits treated with PSLC than in those treated with MPSL, there are studies reporting on ON cases treated with MPSL or PSLC [3, 4, 14, 15]. The occurrence of clinical ON may be influenced by other factors, such as differences in administration methods, corticosteroid doses and underlying diseases [3, 4, 16].

It is difficult to draw a conclusion for human ON from this rabbit experiment due to the interspecies differences. On the basis of the results, we speculate that ON development in humans depends on the type of corticosteroid used; use of an optimal type of corticosteroid would be beneficial for patients with a high risk of ON. This hypothesis may be supported by the presence of several similarities between human and rabbit ON. First, increased lipid deposition and a rise in intraosseous pressure were reported in ON of both species [17–19]. Secondly, histological features of empty lacunae accompanied by surrounding marrow cell necrosis were shared in human and rabbit ON [8, 20]. Thirdly, ON is multifocal in both species [1, 8]. Fourth, haematological risk factors representing prominent lipid transport to the peripheral tissues were reported in humans and rabbits ON [10, 21].

Small differences in the structure of cortisol and its synthetic analogues result in remarkable differences in drug potency and duration of action [22]. All corticosteroid compounds have a common carbon skeleton. Addition of a 1,2 double bond to the corticosteroid nucleus creates PSL. The 6α-methylation (MPSL) or 9α-fluoride addition with 16-hydroxylation (TR) provides less salt-retaining activity but more glucocorticoid potency [22]. In this study, MPSL treatment produced striking findings differing significantly from those seen following PSL and TR treatment, including a high ON incidence. The precise mechanism for this difference is unknown. The 6α-methylation is the feature unique to MPSL, which may mediate long-term cytolysis [23]. Our observations may also be attributable to this component.

Differential binding capacities of the corticosteroid for albumin- and/or corticosteroid-binding globulin (CBG) may be another possible explanation for the high ON occurrence. Albumin and CBG are the primary corticosteroid-binding proteins that transport cortisol; free (unbound) cortisol is the active molecular form [22, 24]. Decreased protein binding in patients with liver disease and hypoalbuminaemia results in the major

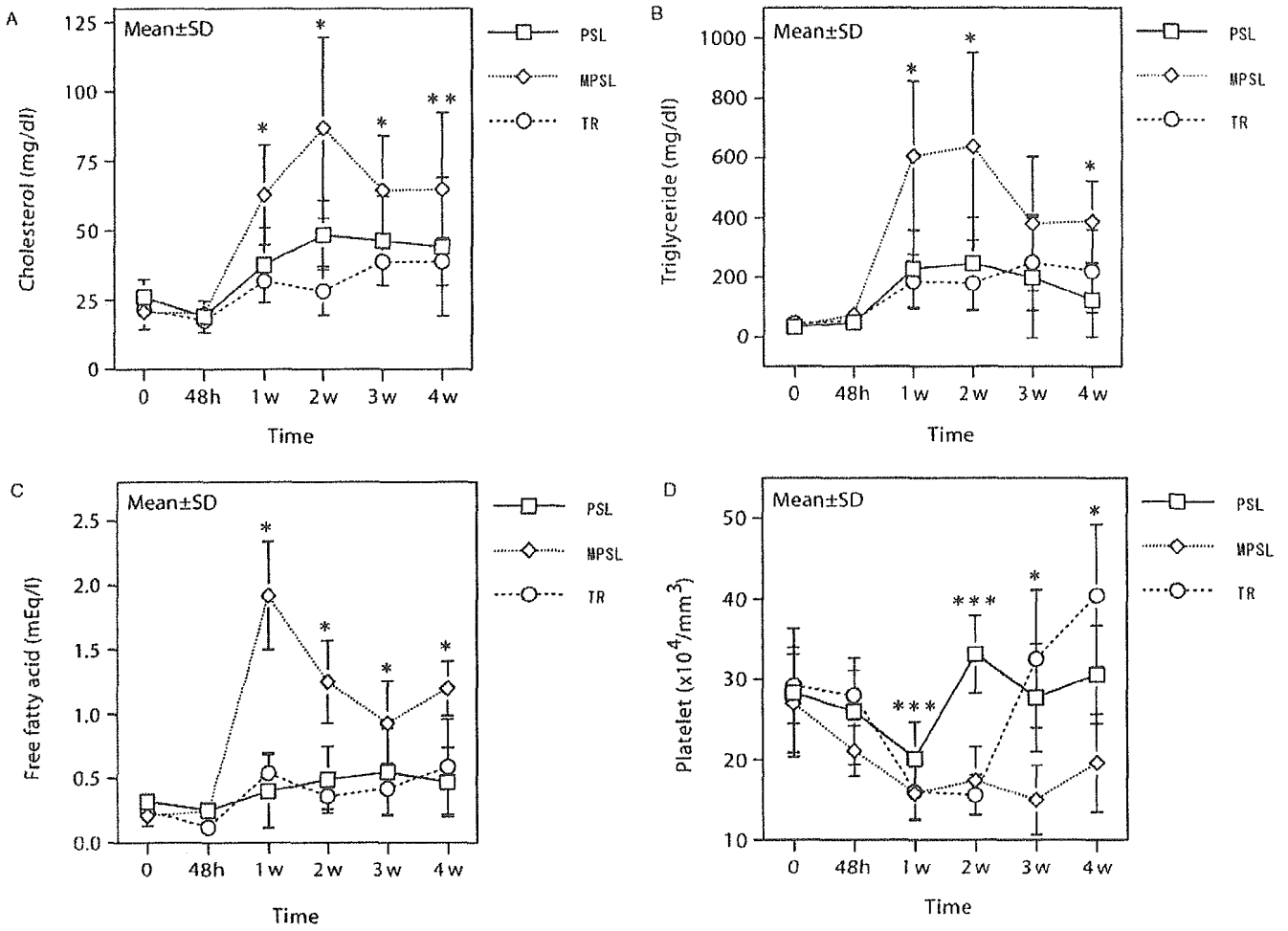

FIG. 2. Sequential changes in the levels of cholesterol (A), triglycerides (B), free fatty acid (C) and platelets (D) in rabbits treated with PSL, MPSL or TR. *$P<0.05$ or 0.01, MPSL *vs* PSL and TR; **$P<0.05$, MPSL *vs* TR; ***$P<0.05$ or 0.01, PSL *vs* MPSL and TR.

side-effects of corticosteroids [25], while increased protein binding may limit the bioactivity of corticosteroids in patients with Crohn's disease [26]. Furthermore, the binding capacity of CBG to MPSL is lower than that to PSL [27]. The decreased binding capacity of CBG to MPSL may increase the free fraction of MPSL, resulting in increased ON incidence.

Coagulation abnormalities and hyperlipidaemia are among the postulated pathogenic mechanisms for ON development [1, 2, 8, 10, 14, 15, 21, 28–30]. Ischaemic events may result from vascular interruption through thrombi, lipid emboli or high intraosseous pressure associated with bone marrow fat-cell enlargement; these processes would subsequently lead to ON development [1, 2, 8, 10, 14, 15, 21, 28–30]. In this study, the platelet levels decreased at 1 week following corticosteroid treatment, suggesting a hypercoagulable plasma state due to increased platelet consumption. The platelet numbers recovered to pretreatment levels at 2 and 3 weeks in rabbits receiving PSL and TR treatment, respectively. However, the platelet levels did not reach pretreatment levels until at least 4 weeks after treatment in MPSL-treated rabbits (Fig. 2D). Significantly increased lipid levels were also observed following MPSL treatment. These data therefore suggest the presence of a hypercoagulable and hyperlipidaemic state of plasma in rabbits treated with MPSL compared with levels seen after PSL or TR treatment. Further study will be needed to clarify the mechanisms for steroid-induced ON, including morphological changes of bone marrow fat cells, the formation of thrombus and fat emboli, and expression of lipid- or coagulation-related genes in the marrow tissues [1, 2, 8, 10, 14, 15, 21, 28–30].

In conclusion, this study demonstrated that MPSL treatment significantly increased the incidence of ON in rabbits, in association with elevated lipid levels, from that observed for PSL or TR treatment. These results suggest that the type of corticosteroid given may be an important component determining human ON development.

Rheumatology	Key messages
	• Development of osteonecrosis in rabbits depended on the type of corticosteroid given. • Use of an optimal type of corticosteroid may be beneficial for patients with a high risk of osteonecrosis.

Acknowledgements

This work was supported in part by a Grant-in-Aid for JSPS Fellows, a Grant for Intractable Diseases from the Ministry of Health and Welfare of Japan and a Grant from Uehara Memorial Foundation.

The authors have declared no conflicts of interest.

References

1. Mankin HJ. Nontraumatic necrosis of bone (osteonecrosis). N Engl J Med 1992;326:1473–9.
2. Lieberman JR, Berry DJ, Mont MA *et al.* Osteonecrosis of the hip: management in the 21st century. Instr Course Lect 2003;52:337–55.
3. Oinuma K, Harada Y, Nawata Y *et al.* Osteonecrosis in patients with systemic lupus erythematosus develops very early after starting high dose corticosteroid treatment. Ann Rheum Dis 2001:60:1145–8.
4. Nagasawa K, Ishii Y, Mayumi T *et al.* Avascular necrosis of bone in systemic lupus erythematosus: possible role of haemostatic abnormalities. Ann Rheum Dis 1989;48:672–6.
5. USPDI. Corticosteroids Glucocorticoid effects (systemic). In: Drug information for the health care professional. Greenwood Village: Micromedex Thomson Healthcare, 2002:1002–27.
6. Badsha H, Edwards CJ. Intravenous pulses of methylprednisolone for systemic lupus erythematosus. Semin Arthritis Rheum 2003;32:370–7.
7. Albert DA, Hadler NM, Ropes MW. Does corticosteroid therapy affect the survival of patients with systemic lupus erythematosus? Arthritis Rheum 1979;22:945–53.
8. Yamamoto T, Irisa T, Sugioka Y, Sueishi K. Effects of pulse methylprednisolone on bone and marrow tissues: corticosteroid-induced osteonecrosis in rabbits. Arthritis Rheum 1997;40:2055–64.
9. Doggrell SA. Triamcinolone: new and old indications. Expert Opin Pharmacother 2001;2:1177–86.
10. Miyanishi K, Yamamoto T, Irisa T *et al.* A high low-density lipoprotein cholesterol to high-density lipoprotein cholesterol ratio as a potential risk factor for corticosteroid-induced osteonecrosis in rabbits. Rheumatology 2001;40:196–201.
11. Melby JC. Drug spotlight program: systemic corticosteroid therapy: pharmacology and endocrinologic considerations. Ann Intern Med 1974;81:505–12.
12. Neidel J, Boehnke M, Kuster RM. The efficacy and safety of intraarticular corticosteroid therapy for coxitis in juvenile rheumatoid arthritis. Arthritis Rheum 2002;46:1620–8.
13. Nasser SMS, Ewan PW. Depot corticosteroid treatment for hay fever causing avascular necrosis of both hips. BMJ 2001;322:1589–91.
14. Jones LC, Mont MA, Le TB *et al.* Procoagulants and osteonecrosis. J Rheumatol 2003;30:783.
15. Mont MA, Glueck CJ, Pacheco IH, Wang P, Hungerford DS, Petri M. Risk factors for osteonecrosis in systemic lupus erythematosus. J Rheumatol 1997;24:654–62.
16. Wing PC, Nance P, Connell DG, Gagnon F. Risk of avascular necrosis following short term megadose methylprednisolone treatment. Spinal Cord 1998;36:633–6.
17. Miyanishi K, Yamamoto T, Irisa T *et al.* Bone marrow fat cell enlargement and a rise in intraosseous pressure in steroid-treated rabbits with osteonecrosis. Bone 2002;30:185–90.
18. Boskey AL, Raggio CL, Bullough PG, Kinnett JG. Changes in the bone tissue lipids in persons with steroid- and alcohol-induced osteonecrosis. Clin Orthop 1983;172:289–95.
19. Zizic TM, Marcoux C, Hungerford DS, Stevens MB. The early diagnosis of ischemic necrosis of bone. Arthritis Rheum 1997; 40:2055–64.
20. Arlet J, Durroux R, Fauchier C, Thiechart M. Histopathology of nontraumatic necrosis of the femoral head: topographic and evolutive aspects. In: Arlet J, Ficat RP, Hungerford DS, eds. Bone Circulation. Baltimore: Williams & Wilkins, 1984:296–305.
21. Miyanishi K, Yamamoto T, Irisa T, Noguchi Y, Sugioka Y, Iwamoto Y. Increased level of apolipoprotein B/apolipoprotein A1 ratio as a potential risk for osteonecrosis. Ann Rheum Dis 1999;58:514–6.
22. Garber EK, Bluestone R. Realistic guidelines of corticosteroid therapy in rheumatic disease. Semin Arthritis Rheum 1981;11: 231–56.
23. Waddell AW, Currie AR. A comparison of the effects of prednisolone and methylprednisolone on human lymphoblastoid cells. Biochem J 1977;168:323–4.
24. Szefler S. General pharmacology. In: Schleimer RP, editor. Anti-inflammatory steroid action of glucocorticoids. San Diego: Academic Press, 1989:353–76.
25. Uribe M, Go VL. Corticosteroid pharmacokinetics in liver disease. Clin Pharmacokinet 1979;4:233–40.
26. Mingrone G, DeGaetano A, Pugeat M, Capristo E, Greco AV, Gasbarrini G. The steroid resistance of Crohn's disease. J Investig Med 1999;47:319–25.
27. Szefler SJ, Ebling WF, Georgitis JW, Jusko WJ. Methylprednisolone versus prednisolone pharmacokinetics in relation to dose in adults. Eur J Clin Pharmacol 1986;30:323–9.
28. Jones JP Jr. Fat embolism, intravascular coagulation, and osteonecrosis. Clin Orthop 1993;292:294–308.
29. Glueck CJ, Freiberg RA, Fontaine RN, Tracy T, Wang P. Hypofibrinolysis, thrombophilia, osteonecrosis. Clin Orthop 2001; 386:19–33.
30. Sheikh JS, Retzinger GS, Hess EV. Association of osteonecrosis in systemic lupus erythematosus with abnormalities of fibrinolysis. Lupus 1998;7:42–8.

Available online at www.sciencedirect.com
SCIENCE DIRECT®
Pathology – Research and Practice 200 (2005) 807–811
PATHOLOGY
RESEARCH AND PRACTICE
www.elsevier.de/prp

ORIGINAL ARTICLE

Bone marrow fat-cell enlargement in early steroid-induced osteonecrosis—a histomorphometric study of autopsy cases

Goro Motomura[a], Takuaki Yamamoto[a,*], Keita Miyanishi[a], Akihisa Yamashita[a], Katsuo Sueishi[b], Yukihide Iwamoto[a]

[a]*Department of Orthopedic Surgery, Graduate School of Medical Sciences, Kyushu University, 3-1-1 Maidashi, Higashi-ku, Fukuoka 812-8582, Japan*
[b]*Division of Pathophysiological and Experimental Pathology, Department of Pathology, Graduate School of Medical Sciences, Kyushu University, 3-1-1 Maidashi, Higashi-ku, Fukuoka 812-8582, Japan*

Received 23 September 2004; accepted 11 October 2004

Abstract

Some animal studies and magnetic resonance imaging studies suggest that there may exist a relationship between abnormal lipid metabolisms and osteonecrosis. The purpose of this study was to examine the size of bone marrow fat cells in the early osteonecrosis femoral head using autopsy specimens.

We compared the size of bone marrow fat cells in the viable areas in the following three autopsy groups: the early osteonecrosis group (4 femoral heads); the steroid-administered group (without osteonecrosis) ($n = 10$), and the normal group ($n = 19$). In addition, after adjusting for age and sex, the size of bone marrow fat cells was compared using multiple regression analysis.

The size of bone marrow fat cells was significantly larger in the early osteonecrosis group ($84.7 \pm 5.5\,\mu m$) than in both the steroid-administered group ($75.3 \pm 4.3\,\mu m$) and the normal group ($76.3 \pm 4.9\,\mu m$) ($p < 0.01$ and $p < 0.05$, respectively). After adjusting for age and sex, the size of bone marrow fat cells in the early osteonecrosis group was significantly larger as compared with the other groups.

This study suggests that in steroid-induced osteonecrosis, the size of bone marrow fat cells increases significantly at an early stage.

Keywords: Ostoenecrosis; Bone marrow fat-cell; Steroid

Introduction

Regarding the pathogenesis of steroid-induced osteonecrosis, reports on an abnormal lipid metabolism are based mainly on the histologic investigations of animal models. Wang et al. reported on a significant increase in the size of bone marrow fat cells in cortisone-treated rabbits [13]. Miyanishi et al. found that the diameter of marrow fat cells was significantly larger in rabbits with osteonecrosis than in those without [5]. On the other hand, investigating humans, Solomon reported on bone marrow fat-cell enlargement in which the stage of osteonecrosis was not clarified [9].

Histologic examinations in early stage (asymptomatic stage) osteonecrosis is one of the most useful methods for investigating the pathogenesis of osteonecrosis, because at an advanced stage, it is often difficult to

*Corresponding author. Tel.: +81 92 642 5488; fax: +81 92 642 5507.
E-mail address: yamataku@ortho.med.kyushu-u.ac.jp (T. Yamamoto).

0344-0338/$ - see front matter © 2004 Elsevier GmbH. All rights reserved.
doi:10.1016/j.prp.2004.10.003

judge whether the histologic alterations are primary changes or the result of collapses and the following repair processes. However, there are only few opportunities to examine histopathologically whole femoral heads affected by osteonecrosis in the early, asymptomatic stage. To the best of our knowledge, there exists only one documentation of a case that has described the histopathologic findings of early osteonecrosis [10]. For this, a whole femoral head obtained at autopsy was used.

Over the past 10 years, we have had the opportunity to examine four whole femoral heads with early (asymptomatic) stage steroid-induced osteonecrosis (Association of Research Circulation Osseous (ARCO) stage 1 [11]) obtained at autopsy. In this study, we investigated these whole femoral heads to ascertain whether bone marrow fat cells increase in size at an early stage of osteonecrosis.

Patients and methods

Patients

The four whole femoral heads were obtained from four patients affected by steroid-induced osteonecrosis in ARCO stage 1 (early osteonecrosis group). All of these four cases, belonging to the early osteonecrosis group, were obtained at autopsy within 12 h after death. The cases were collected over a period of 10 years, and the patients had received high dosages of corticosteroids (peak dose of prednisolone: 40–1000 mg). None of the patients had any symptoms in the hip, but osteonecrosis was diagnosed on the basis of the published histologic criteria [2,8,16].

Regarding the control groups, 29 femoral heads were obtained from 29 patients at autopsies done within 12 h after death, also collected over the period of 10 years. Ten patients had a history of high dosage corticosteroids administration (peak dose of prednisolone: 25–1000 mg), but without histologic evidence of osteonecrosis (steroid-administered group). There were 19 patients who had neither a history of corticosteroid treatment nor any hip disorder (normal group).

Patients taking drugs to affect the lipid metabolism and/or who had been bedridden for more than 1 week were excluded from this study. None of the patients had a history of alcohol abuse.

All the patients or the family members of every autopsied case gave their consent to the publication of patient data.

Tissue preparation

The corpses were stored in a mortuary at 4 °C until autopsy. The mean storage time was 4 h (range 2–12 h).

Thereafter, the whole femoral heads were removed and fixed in a 10% formalin solution for 1 week. They were then cut into serial 2 mm stepwise sections, vertically to the long axis of the femoral neck. Each section was delipidized in a 1:1 chloroform methanol mixture for 2 h, dehydrated in a 75% ethanol solution for 2 days, and decalcified with a 25% formic acid solution for 7 days, followed by neutralization with sodium sulfate. Finally, all the sections were stained with hematoxylin and eosin.

Bone marrow fat-cell measurements

The size of bone marrow fat cells was measured on the basis of viable areas (the osteonecrotic lesion was excluded from this measurement). As described in a previous report [5,13], the size of bone marrow fat cells in one femoral head was calculated as the average of the greatest diameters of 100 fat cells in four randomly selected fields (1 field $= 41 \times 10^{-8}\,m^2$) using the NIH image soft package. Briefly, a camera was used that sent electronically an image of the sections to an image processor. The greatest diameter of the bone marrow fat cells displayed on the video monitor was measured using an interactive mousepad-tracing instrument. The corresponding morphometric data were then processed automatically by a computer system.

Repeatability of measurements of fat-cell size

The repeatability of the bone marrow fat-cell measurements was determined by two authors (GM and TY) measuring these values in the 33 femoral heads on two occasions in a 1-week interval [1]. The interobserver differences (the differences between the measurements by GM and those by TY for each femoral head) were regarded as the mean values of differences in all femoral heads. The intraobserver differences (the differences between two measurements taken at different times by GM for the same femoral head) were considered to be the mean values of differences in all femoral heads. The interobserver and intraobserver coefficients of repeatability were also calculated.

Statistical analysis

Data were expressed as the mean ± standard deviation. Among the three groups, the size of bone marrow fat cells was compared using one-way analysis of variance (ANOVA) with the Scheffe post hoc test. Between the steroid-treated groups (early osteonecrosis group and steroid-administered group), both the time interval (between steroid administration and removal of the femoral head) and the peak dose of prednisolone (which has been reported to affect the development of

steroid-induced osteonecrosis [6,7]) were compared using Mann–Whitney's *U*-test.

To adjust the size of bone marrow fat cells for age and sex, multiple regression analysis was performed, in which the size of bone marrow fat cells was the dependent variable. For two groups (steroid-administered group and normal group), which are explanatory variables, we used a method for creating dummy variables [3]. The reference group was the early osteonecrosis group.

Statistical analyses were performed using StatView J-5.0 (SAS Institute Inc, Cary, NC, USA). Statistical differences were considered to be significant when the p value was less than 0.05.

Results

Patients (Table 1)

In the early osteonecrosis group, the mean age at the time of death was 41 years (range 33–47 years). This group consisted of three women and one man, two of whom were treated for systemic lupus erythematosus, one for biliary cirrhosis, and one for cholangitis. In the steroid-administered group, the mean age at the time of death was 55.8 years (range 38–77 years); there were eight men and two women, and eight were treated for blood disorders, one for periarteritis nodosa, and one for another disease. In the normal group, the mean age at the time of death was 56.7 years (range 32–76 years). This group was composed of 13 men and six women, and 13 were treated for malignant tumors, three for heart disease, and three for other diseases.

The steroid-treated groups (the early osteonecrosis and the steroid-administered groups) differed with regard to the mean (±standard deviation) peak dose of prednisolone (the early osteonecrosis group: 351 ± 451 mg, the steroid-administered group: 247 ± 398 mg), but this difference was not statistically significant ($p = 0.56$). There was also no significant difference in the time interval (between steroid administration and removal of the femoral head; early osteonecrosis group: 30 ± 52 months, steroid-administered group: 21 ± 34 months).

Fat-cell size

The size of bone marrow fat cells was 84.7 ± 5.5, 75.3 ± 4.3 and 76.3 ± 4.9 μm in the early osteonecrosis, steroid-administered, and normal groups, respectively. Among the groups, the size of bone marrow fat cells was significantly larger in the early osteonecrosis group than in the control groups (steroid-administered group and normal group) ($p < 0.01$ and $p < 0.05$, respectively) (Figs. 1 and 2).

Multiple regression analysis revealed that the size of bone marrow fat-cells was significantly larger in the early osteonecrosis group than in both the steroid-administered group ($p = 0.0003$) and the normal Group ($p = 0.0003$), even after adjusting age and sex (Table 2), the size of bone marrow fat cells being a dependent variable, and age, sex (male = 0, female = 1), and groups (dummy variable) representing independent variables.

The mean interobserver and intraobserver differences of the fat-cell size were 3.70 μm (range −3.75–9.50; 95% confidence interval, 1.93–5.47) and 0.79 μm (range, −6.50–6.38; 95% confidence interval, −0.72–2.31), respectively. The interobserver and intraobserver coefficients of repeatability were 7.37 and 6.31 μm, respectively.

Discussion

The major limitation of this study is the small number of early osteonecrosis cases ($n = 4$). However, except for biopsy cases, there are only few opportunities that allow for the examination of whole femoral heads affected by osteonecrosis at an early, asymptomatic stage. Although

Table 1. Cinical profile in every group

Group	Age[a] (years)	Sex	Underlying disease	Mean peak dose of prednisolone (mg)	Time interval[b] (months)
Early osteonecrosis	41.0 (33–47)	1M3F	SLE 2, Biliary cirrhosis 1, Cholangitis 1	351 (40–1000)	30 (2–108)
Steroid-administered	55.8 (38–77)	8M2F	Blood disorder 8, PN1, others 1	247 (25–1000)	21 (2–116)
Normal	56.7 (32–76)	13M6F	Malignant tumor 13, heart disease 3, others 3	—	—

SLE: systemic lupus erythematosus, PN: Periarteritis nodosa.
[a]mean age at the time of death.
[b]mean time interval between steroid administration and removal of femoral head.

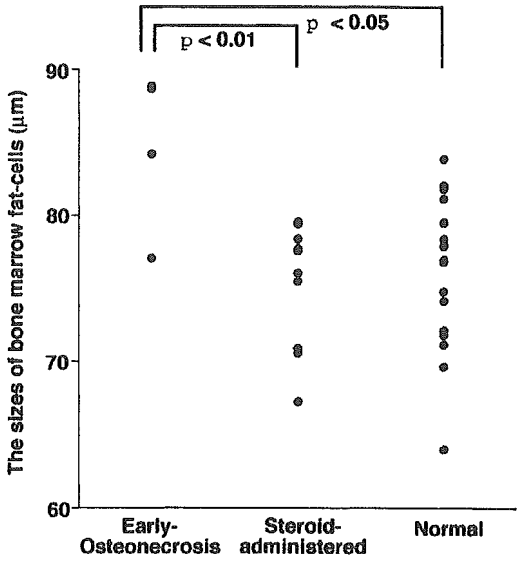

Fig. 1. The size of bone marrow fat-cells (μm). The size of marrow fat cells was significantly larger in the early osteonecrosis group (84.7±5.5 μm) than in both the steroid-administered group (without osteonecrosis) (75.3±4.3 μm) and the normal group (76.3±4.9 μm) ($p<0.01$ and $p<0.05$, respectively). There were no significant differences between the steroid-administered group and the normal group.

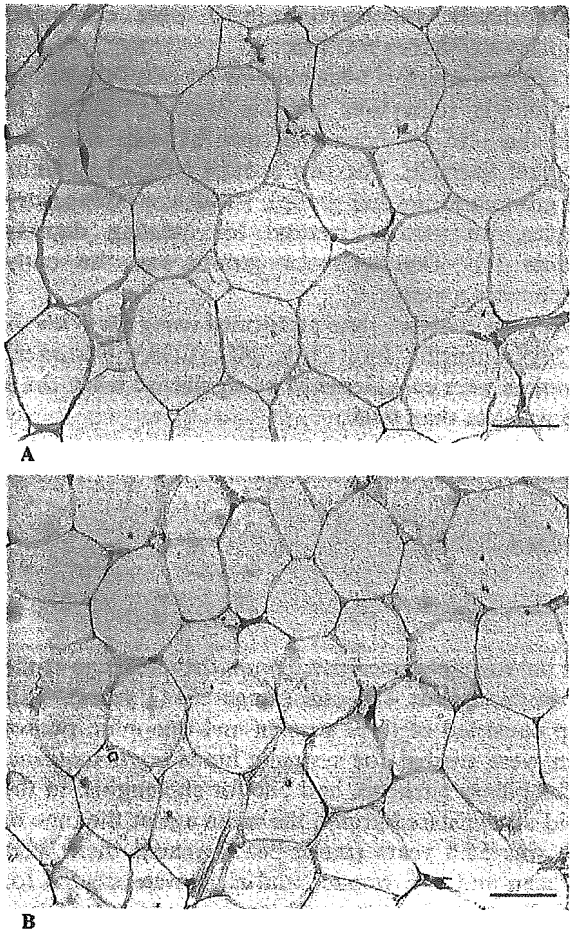

Fig. 2. Histopathologic appearance of bone marrow fat cells in the femoral head. (A) Early osteonecrosis case (early osteonecrosis group). A 40-year-old woman received steroids (peak dose of prednisolone: 40 mg) with treatment starting 2 months before death. The mean size of 100 bone marrow fat cells was 88.7 μm. (B) Steroid-administered case without osteonecrosis (steroid-administered group). A 50-year-old man received steroids (peak dose of prednisolone: 40 mg) with treatment starting 3 months before death. The mean size of 100 bone marrow fat cells was 79.4 μm (hematoxylin- and eosin-stained; original magnification ×200; bar = 50 μm).

we evaluated only four cases at an early stage, we believe that a careful statistical examination of these cases is meaningful as long as some significant values are noted between the groups.

The present study suggests that in steroid-induced osteonecrosis, the size of bone marrow fat cells enlarges at an early stage, which supports the observations made in previous animal studies. In a rabbit model of steroid-induced osteonecrosis, the size of bone marrow fat cells in rabbits with osteonecrosis increased within 2 weeks after steroid administration, and this point of time is reported to be crucial for the development of osteonecrosis [5,15].

A recent magnetic resonance imaging (MRI) study showed that steroid-treated patients with MRI-detected osteonecrotic lesions had a more pronounced increase in marrow fat than steroid-treated patients without osteonecrosis [12]. As the enlargement of bone marrow fat cells contributes to the conversion of hematopoietic marrow into fatty marrow [5,13], this MRI finding seems to be consistent with our results that the size of bone marrow fat cells in early steroid-induced osteonecrosis (early osteonecrosis group) was significantly larger than in cases without osteonecrosis (steroid-administered group). We presume that cases with a high sensitivity to steroids seem to be vulnerable to an increase in the bone marrow fat-cell size, which may result in conversion into fatty marrow.

In one patient in the early osteonecrosis group, the time interval between steroid administration and removal of the femoral head was 108 months (9 years). This fact implies that in this case, osteonecrosis is not in its early phase. However, histologically, the subchondral bone was characterized by necrotic bone and bone marrow tissue with granular appearance and infiltration of inflammatory cells, without a layer of new bone on the pre-existing dead bone. These characteristic findings indicate that in this case, osteonecrosis was in its early phase [2,8,16].

It is controversial whether the enlargement of bone marrow fat cells in patients with osteonecrosis is a result

Table 2. Multiple regression analysis for the comparison with early-osteonecrosis group after adjusting for age and sex

Independent variables	Regression coefficients	Standard error	p
Age	0.127	0.066	0.0671
Sex	−2.425	1.788	0.1859
Steroid-administered group	−11.283	3.316	0.0003
Normal group	−10.189	3.093	0.0003
	$R^2 = 0.405$, $F_{4,28} = 4.763$, $p = 0.0047$		

of osteonecrosis. In the present study, we measured the size of bone marrow fat cells in the viable area of the femoral head affected by early osteonecrosis in the same manner as in the previous animal study [5]. Therefore, we believe that the enlarged bone marrow fat cells in the viable area may not be affected by osteonecrosis, but presumably precede the development of osteonecrosis.

It is still unclear whether a causative relationship exists among the factors of enlarged bone marrow fat cells, ischemia, and resultant osteonecrosis. We do not believe that fat cell enlargement alone is the only important event associated with osteonecrosis. Steroids have been reported to induce a hypercoagulable and hypofibrinolytic state of the blood, arteriopathy, and an enlargement of fat cells [4,14]. Therefore, the pathogenesis of osteonecrosis still needs to be verified.

In summary, the size of bone marrow fat cells enlarge in human early steroid-induced osteonecrosis.

Acknowledgement

This work is supported in part by a Research Grant for Intractable Diseases from the Ministry of Health, Labor, and Welfare of Japan, and a Grant-in-Aid in Scientific Research (No. 15591587) from JSPS. We would like to thank Naoko Kinukawa (Department of Medical Informatics, Kyushu University, Fukuoka, Japan) for her helpful advice on the statistical analysis.

References

[1] J.M. Bland, D.G. Altman, Statistical methods for assessing agreement between two methods of clinical measurement, Lancet 1 (1986) 307–310.
[2] P.G. Bullough, E.F. DiCarlo, Subchondral avascular necrosis: a common cause of arthritis, Ann. Rheum. Dis. 49 (1990) 412–420.
[3] W.J. Dixon, BMDP Statistical Software Manual, University of California Press, Berkeley, 1992, pp. 1145–1180.
[4] M. Matsui, S. Saito, K. Ohzono, N. Sugano, M. Saito, K. Takaoka, K. Ono, Experimental steroid-induced osteonecrosis in adult rabbits with hypersensitivity vasculitis, Clin. Orthop. 277 (1992) 61–72.
[5] K. Miyanishi, T. Yamamoto, T. Irisa, A. Yamashita, S. Jingushi, Y. Noguchi, Y. Iwamoto, Bone marrow fat cell enlargement and a rise in intraosseous pressure in steroid-treated rabbits with osteonecrosis, Bone 30 (2002) 185–190.
[6] C.C. Mok, C.S. Lau, R.W. Wong, Risk factors for avascular bone necrosis in systemic lupus erythematosus, Br. J. Rheumatol. 37 (1998) 895–900.
[7] M.A. Mont, C.J. Glueck, I.H. Pacheco, P. Wang, D.S. Hungerford, M. Petri, Risk factors for osteonecrosis in systemic lupus eryhematosus, J. Rheumatol. 24 (1997) 654–662.
[8] H.A. Sissons, M.A. Nuovo, G.C. Steiner, Pathology of osteonecrosis of the femoral head. A review of experience at the Hospital for Joint Diseases, New York, Skeletal Radiol. 21 (1992) 229–238.
[9] L. Solomon, Idiopathic necrosis of the femoral head: pathogenesis and treatment, Can. J. Surg. 24 (1981) 573–578.
[10] J.D. Spencer, S. Humphreys, J.R. Tighe, R.R. Cumming, Early avascular necrosis of the femoral head. Report of a case and review of the literature, J. Bone Joint Surg. Br. 68 (1986) 414–417.
[11] B. Stulberg, Editorial comment, Clin. Orthop. 334 (1997) 2–5.
[12] B.C. Vande Berg, J. Malghem, F.E. Lecouvet, J.P. Devogelaer, B. Maldague, F.A. Houssiau, Fat conversion of femoral marrow in glucocorticoid-treated patients: a cross-sectional and longitudinal study with magnetic resonance imaging, Arthritis Rheum. 42 (1999) 1405–1411.
[13] G.J. Wang, D.E. Sweet, S.I. Reger, R.C. Thompson, Fat-cell changes as a mechanism of avascular necrosis of the femoral head in cortisone-treated rabbits, J. Bone Joint Surg. Am. 59 (1977) 729–735.
[14] T. Yamamoto, K. Hirano, H. Tsutsui, Y. Sugioka, K. Sueishi, Corticosteroid enhances the experimental induction of osteonecrosis in rabbits with Shwartzman reaction, Clin. Orthop. 316 (1995) 235–243.
[15] T. Yamamoto, T. Irisa, Y. Sugioka, K. Sueishi, Effects of pulse methylprednisolone on bone and marrow tissues: corticosteroid-induced osteonecrosis in rabbits, Arthritis Rheum. 40 (1997) 2055–2064.
[16] T. Yamamoto, E.F. DiCarlo, P.G. Bullough, The prevalence and clinicopathological appearance of extension of osteonecrosis in the femoral head, J. Bone Joint Surg. Br. 81 (1999) 328–332.

British Journal of Pharmacology (2005) 146, 25–32
www.nature.com/bjp

The effects of flavoxate hydrochloride on voltage-dependent L-type Ca^{2+} currents in human urinary bladder

[1,2]Toshihisa Tomoda, [1,2]Manami Aishima, [2]Naruaki Takano, [3]Toshiaki Nakano, [2]Narihito Seki, [3]Yoshikazu Yonemitsu, [3]Katsuo Sueishi, [2]Seiji Naito, [1]Yushi Ito & *,[1]Noriyoshi Teramoto

[1]Department of Pharmacology, Graduate School of Medical Sciences, Kyushu University, Fukuoka 812-8582, Japan; [2]Department of Urology, Graduate School of Medical Sciences, Kyushu University, Fukuoka 812-8582, Japan and [3]Division of Pathophysiological and Experimental Pathology, Graduate School of Medical Sciences, Kyushu University, Fukuoka 812-8582, Japan

1 The effects of flavoxate hydrochloride (Bladderon®, piperidinoethyl-3-methylflavone-8-carboxylate; hereafter referred as flavoxate) on voltage-dependent nifedipine-sensitive inward Ba^{2+} currents in human detrusor myocytes were investigated using a conventional whole-cell patch-clamp. Tension measurement was also performed to study the effects of flavoxate on K^+-induced contraction in human urinary bladder.

2 Flavoxate caused a concentration-dependent reduction of the K^+-induced contraction of human urinary bladder.

3 In human detrusor myocytes, flavoxate inhibited the peak amplitude of voltage-dependent nifedipine-sensitive inward Ba^{2+} currents in a voltage- and concentration-dependent manner ($K_i = 10\,\mu M$), and shifted the steady-state inactivation curve of Ba^{2+} currents to the left at a holding potential of −90 mV.

4 Immunohistochemical studies indicated the presence of the α_{1C} subunit protein, which is a constituent of human L-type Ca^{2+} channels ($Ca_V1.2$), in the bundles of human detrusor smooth muscle.

5 These results suggest that flavoxate caused muscle relaxation through the inhibition of L-type Ca^{2+} channels in human detrusor.

British Journal of Pharmacology (2005) **146**, 25–32. doi:10.1038/sj.bjp.0706284; published online 20 June 2005

Keywords: Flavoxate; frequency of micturition; human detrusor myocytes; L-type Ca^{2+} channels; overactive bladder; spasmolytic agent

Abbreviations: CNS, central nervous system; DHP, dihydropyridine; DMSO, dimethyl sulphoxide; flavoxate hydrochloride, piperidinoethyl-3-methylflavone-8-carboxylate hydrochloride; OAB, overactive bladder; PBS, phosphate-buffered saline; PSS, physiological salt solution; TEA^+, tetraethylammonium

Introduction

Since the synthesis of flavoxate (piperidinoethyl-3-methylflavone-8-carboxylate hydrochloride) and its introduction to the urological field (Kohler & Morales, 1968), it has been widely used to treat urge frequency of micturition (i.e., urgency) for more than three decades (reviewed by Haeusler *et al.*, 2002).

Flavoxate acts centrally to suppress the micturition reflex (Kaseda *et al.*, 1975; Yoshimura *et al.*, 1992). It has also been reported that flavoxate increases urinary bladder capacity, by modifying the micturition centre in the brain stem (Kimura *et al.*, 1996), and that flavoxate inhibits cyclic AMP formation in rat striatal membranes of the brain through the stimulation of pertussis toxin-sensitive G protein-coupled receptors, which in turn suppresses isovolumetric rhythmic urinary bladder contraction (Oka *et al.*, 1996). Thus, it has been generally thought that the beneficial effects of flavoxate for urinary frequency are through modulation of the central nervous system (CNS) control of micturition.

On the other hand, there are several reports that flavoxate causes a significant relaxation of urinary bladder smooth muscle precontracted by carbacol or electrical field stimulation (rat, Kimura *et al.* (1996); human, Uckert *et al.*, 2000). These results strongly indicate that flavoxate possesses direct inhibitory effects on the detrusor muscle in addition to the actions on the CNS. However, the precise mechanisms involved in the flavoxate-induced detrusor relaxation remain elusive, and the target channels for flavoxate in the detrusor smooth muscle have not yet been identified.

It is well documented that voltage-dependent Ca^{2+} channels play an important role as a Ca^{2+} influx pathway, which initiates the contraction of smooth muscle cells (reviewed by McFadzean & Gibson, 2002). In the present experiments, therefore, we have first studied the effects of flavoxate on K^+-induced tension using strips prepared from human urinary bladder. Second, we have investigated the effects of flavoxate on voltage-dependent nifedipine-sensitive Ba^{2+} currents (i.e., L-type Ca^{2+} currents or $Ca_V1.2$) in single freshly dispersed

*Author for correspondence at: Department of Pharmacology, Graduate School of Medical Sciences, Kyushu University, 3-1-1 Maidashi, Higashi Ward, Fukuoka 812-8582, Japan; E-mail: noritera@linne.med.kyushu-u.ac.jp

detrusor smooth muscle myocytes from human bladder, by use of whole-cell patch-clamp techniques.

Methods

Tension measurement and data analysis

Small segments of human detrusor was obtained from patients (a total of 27 patients, 39–81 years old; average age, 66 years old) with a stable urinary bladder who were generally undergoing cystectomy for bladder cancer after informed patient consent and with ethical approval from the Kyushu University Hospital Ethical Committee (Fukuoka, Japan). A segment of detrusor was excised and quickly transferred into modified physiological salt solution (PSS) as described previously (Teramoto *et al.*, 2001). An initial tension equivalent to 0.5 g weight was applied to each human detrusor strip, which was then allowed to equilibrate for approximately 1 h until the basal tone became stable (36–37°C). Data were recorded on a Macintosh computer (Macintosh G4, Apple Computer, Tokyo, Japan), through 'MacLab 3.5.6' (AD-Instruments Pty Ltd, Castle Hill, Australia). The tension was expressed as $mN\,mg^{-1}$ of tissue.

Cell preparation and patch-clamp experiments recording procedure

We used freshly dispersed single detrusor myocytes prepared from human urinary bladder. We employed the cell dispersion method previously described (the gentle tapping method; Teramoto & Brading, 1996). The set-up of the patch-clamp experimental system used was essentially the same as described previously (Teramoto *et al.*, 2003). All experiments were performed at room temperature (21–23°C).

Data analysis

The whole-cell current data were low-pass filtered at 500 Hz (−3 dB) by an eight-pole Bessel filter (NF Electronic Instruments, Yokohama, Japan), sampled at 1 ms and analysed on a computer (Macintosh G4, Apple Computer, Tokyo, Japan) by use of the commercial software 'Mac Lab 3.5.6' (ADInstruments Pty Ltd, Castle Hill, Australia). The dissociation constant for drug binding to the inactivated state of the channel could be estimated from the shift of the voltage-dependent inactivation curve and the concentration–response curve obtained at the resting state by using the following equation (Uehara & Hume, 1985):

$$-\Delta V_{half} = k \ln\{(1 + [D]/K_{inact})/(1 + [D]/K_{rest})\}$$

where ΔV_{half} is the amplitude of the shift of the voltage-dependence of the activation curve, k is a slope factor for the inactivation curve and [D] is the concentration of drug applied. K_{inact} and K_{rest} are dissociation constants of flavoxate for the inactivated and the resting states of voltage-dependent Ba^{2+} channels, respectively.

Solutions and drugs

Modified PSS (mM): Na^+ 140, K^+ 5, Mg^{2+} 1.2, Ca^{2+} 2, Cl^- 151.4, glucose 10, HEPES 10, titrated to pH 7.35–7.40 with Tris base. For recording voltage-dependent Ba^{2+} currents in whole-cell configuration, high caesium pipette solution contained (mM): Cs^+ 130, tetraethylammonium (TEA^+) 10, Mg^{2+} 2, Cl^- 144, glucose 5, EGTA 5, ATP 5, HEPES 10/Tris (pH 7.35–7.40). Ba^{2+} 10 mM bath solution contained (mM): Ba^{2+} 10, TEA^+ 135, Cl^- 155, glucose 10, HEPES 10/Tris (pH 7.35–7.40). Cells were allowed to settle in the small experimental chamber (approximately 80 μl in volume). The bath solution was superfused by gravity throughout the experiments at a rate of $2\,ml\,min^{-1}$. Flavoxate hydrochloride (kindly provided by Nippon Shinyaku, Kyoto, Japan) was prepared daily as 100 mM stock solutions in dimethyl sulphoxide (DMSO). The rest of the chemicals were purchased from Sigma (Sigma Chemical K.K., Tokyo, Japan). The final concentration of DMSO was less than 0.3%, not affecting membrane currents.

Immunohistochemical studies

Tissue samples from human urinary bladder were embedded in OCT compound (Tissues-Tek, SAKURA, Tokyo, Japan) in disposable plastic tubes and rapidly frozen in liquid nitrogen. Sections were cut in a cryostat (Leica, CM3050 S, Tokyo, Japan) at a thickness of 6 μm and mounted on silane-precoated glass slides, then allowed to air dry at room temperature for approximately 30 min. Sections were fixed in cold acetone and washed thoroughly in phosphate-buffered saline (PBS) before staining. The tissue sections were treated in 3% nonfat milk (Bean Stalk Snow Co. Ltd, Sapporo, Japan) in PBS, and then reacted with the primary antibody, polyclonal rabbit anti-$Ca_V1.2$ (α_{1C}) ACC-003 antibody (diluted at 1 : 400, Alomone Labs, Jelsalem, Israel; Péréon *et al.*, 1998) at 4°C overnight. Sections were then washed for 3 × 5 min in PBS. Visualization was achieved by subsequent incubation in biotinylated goat-anti-rabbit IgG (Histofine secondary antibody, Nichirei, Tokyo, Japan) for 30 min, followed by phycoerythrin-labelled avidin–biotin complex reagent (Streptavidin–phycoerythrin, BD pharmingen, Franklin Lakes, NJ, U.S.A.) for 30 min at room temperature under dark conditions. Sections were then washed for 3 × 5 min in PBS. Coverslips were mounted onto slides by use of fluorescence mounting medium and slides viewed by fluorescent microscopy (Olympus BX51, Olympus Optical Co. Ltd, Tokyo, Japan). Absorption test was performed by utilizing antiboby that had been preincubated with the control peptide antigen (residues 848–865 of rat α_{1C}, P22002). Nonimmunized rabbit IgG was also used instead of primary antibody for a negative control.

Statistical analysis

Statistical analyses were performed with analysis of variance (ANOVA) test (two-factor with replication). Changes were considered significant at $P<0.05$ (*).

Results

Effects of flavoxate on K^+-induced contraction

Tension measurement was performed to investigate the effects of flavoxate on K^+ (10, 20, 40 and 80 mM)-induced contraction of human urinary bladder (Figure 1). Application of high K^+ solution (2 min duration) caused a contraction in a

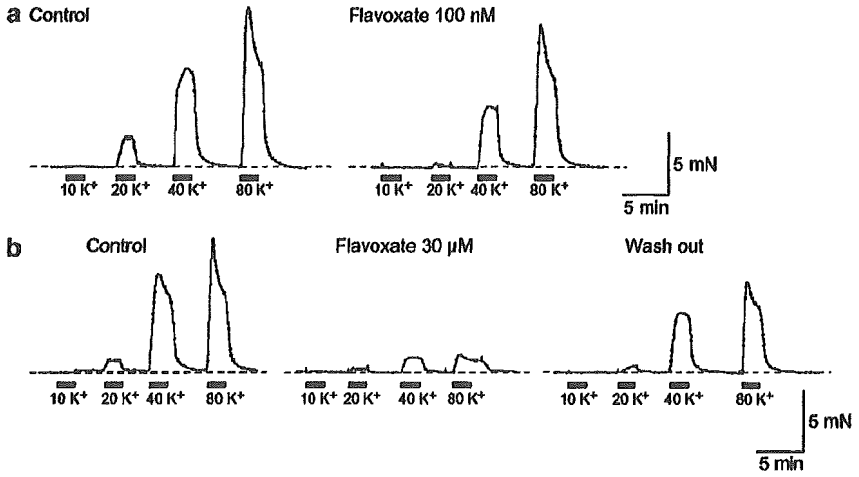

Figure 1 Effects of flavoxate on K^+-induced contraction (10, 20, 40 and 80 mM) of human detrusor strips. (a) K^+-induced contraction in the absence (control) and presence of 100 nM flavoxate. (b) K^+-induced contraction in the absence and presence of 30 μM flavoxate.

concentration-dependent manner. Flavoxate (100 nM) suppressed the amplitude of K^+-induced contraction. At 30 μM, flavoxate inhibited the K^+-induced contraction over the full range of K^+ concentrations from 20 to 80 mM. After approximately 30 min washout of flavoxate, the K^+-induced contraction was partially recovered but did not return to the control level. Figure 2 summarizes these results. The relative value of each K^+-induced contraction was obtained when the peak amplitude of 80 mM K^+-induced contraction in the absence of flavoxate was normalized as one.

Voltage-dependent Ca^{2+} currents

It was previously reported that the peak amplitude of nifedipine-sensitive voltage-dependent Ca^{2+} currents in human detrusor was too small to estimate precisely (Kajioka *et al.*, 2002). Thus, in the present experiments, Ba^{2+} (10 mM) was used as a charge carrier in the bath solution in order to enhance the amplitude of the inward currents for analysis and to isolate voltage-dependent inward Ca^{2+} currents by inhibiting other Ca^{2+}-activated mechanisms (such as Ca^{2+}-activated K^+ currents and Ca^{2+}-activated Cl^- currents, etc.). The recording pipette was filled with a Cs^+-TEA^+ solution containing 5 mM EGTA.

Application of a depolarizing step to +10 mV from a holding potential of −60 mV produced an inward Ba^{2+} current (Figure 3a(i)). This current increased slightly with time after establishing the whole-cell configuration, reaching a steady state approximately 4 min after rupture of the membrane patch ($n=60$). This peak value was then maintained at least for 15 min if test depolarization pulses (1 s duration) were applied at 20 s intervals (the peak amplitude of the voltage-dependent Ba^{2+} current at 15 min being 98±2% ($n=10$) of the value determined 4 min after establishment of a conventional whole-cell recordings). Consequently, all experiments were performed within this 15 min period.

Effects of flavoxate on voltage-dependent Ba^{2+} inward currents

Figure 3b shows the time course of the effects of flavoxate (10 μM) on the Ba^{2+} inward current. Application of flavoxate

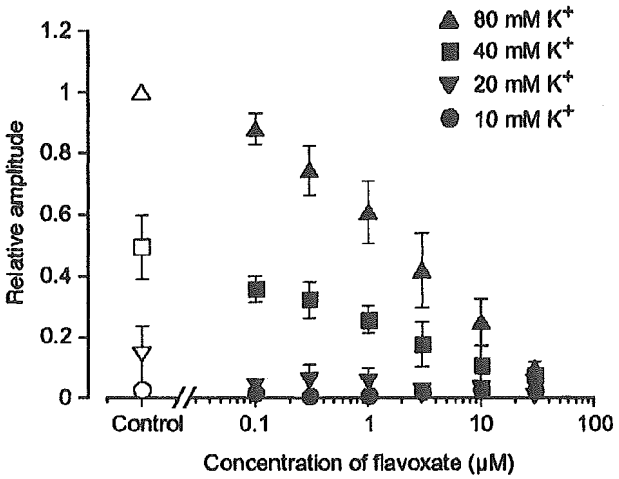

Figure 2 Effects of flavoxate (⩾100 nM) on the peak amplitude of K^+-induced contraction of human detrusor strips, when the peak amplitude of 80 mM K^+-induced contraction in the absence of flavoxate was normalized as one.

(10 μM) gradually reduced the peak amplitude of the inward current and nearly halved it within a few min (0.49±0.1, $n=5$). Subsequent application of nifedipine (10 μM) completely suppressed the currents. Figure 4 shows the relationships between the relative peak amplitude of Ba^{2+} inward currents evoked by a depolarizing pulse to +10 mV from two different holding potentials (−60 and −90 mV) applied every 20 s and concentrations of flavoxate. Flavoxate inhibited the peak amplitude of the Ba^{2+} inward currents in a concentration-dependent manner (−60 mV, $K_i=10$ μM; −90 mV, $K_i=56$ μM).

Voltage-dependent inhibitory effects of flavoxate on voltage-dependent Ba^{2+} currents

As shown in Figure 5a, flavoxate inhibited the peak amplitude of the Ba^{2+} currents evoked by depolarizing pulses (1 s duration) from a holding potential of −60 mV at levels more

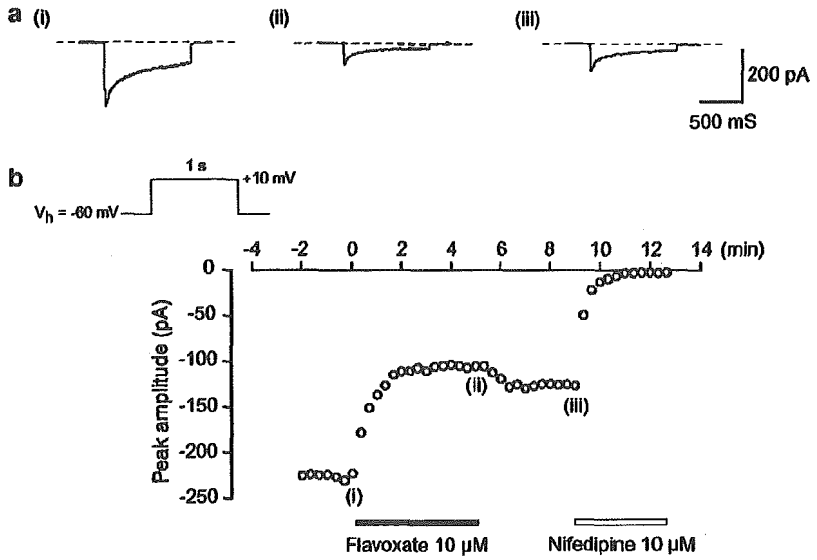

Figure 3 Effects of flavoxate and nifedipine on voltage-dependent Ba^{2+} currents in human detrusor. Whole-cell recording, pipette solution Cs^+-TEA^+ solution containing 5 mM EGTA and bath solution 10 mM Ba^{2+} containing 135 mM TEA^+. (a) Original current traces before (control, (i)) and after application of 10 μM flavoxate (ii), as indicated in (b). (iii) Indicates a current trace just before the application of 10 μM nifedipine. (b) The time course of the effects of application of flavoxate and nifedipine on the peak amplitude of the voltage-dependent Ba^{2+} current evoked by repetitive depolarizing pulses to +10 mV from a holding potential of −60 mV. Time 0 indicates the time when 10 μM flavoxate was applied to the bath.

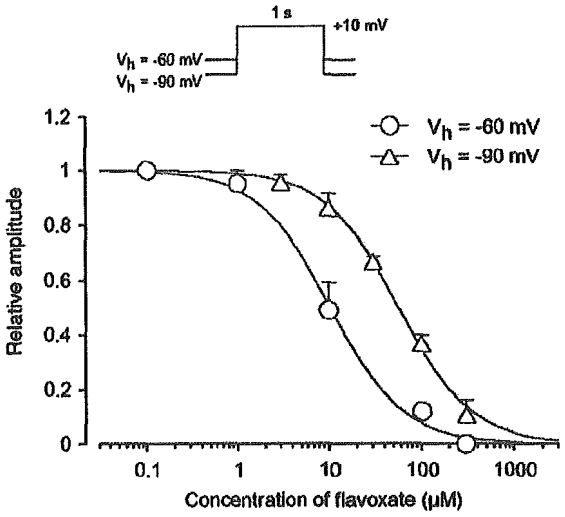

Figure 4 Concentration–response curves for flavoxate on voltage-dependent Ba^{2+} currents in human detrusor. Relationships between relative inhibition of the peak amplitude of Ba^{2+} current and the concentration of flavoxate at two holding potentials (−60 and −90 mV). The peak amplitude of the Ba^{2+} current elicited by a step pulse to +10 mV from the holding potential just before application of flavoxate was normalized as one. The curves were drawn by fitting the following equation using the least-squares method: Relative amplitude of voltage-dependent Ba^{2+} current $= 1/\{1 + (D/K_i)\ n_H\}$ where K_i, D and n_H are the inhibitory dissociation constant, concentration of flavoxate (μM) and Hill's coefficient, respectively. The following values were used for the curve fitting: −60 mV, $K_i = 10\ \mu$M, $n_H = 1.1$; −90 mV, $K_i = 56\ \mu$M, $n_H = 1.1$. Each symbol indicates the mean of 5–15 observation with ± s.d. shown by vertical lines. Some of the s.d. bars are less than the size of the symbol.

positive than −30 mV. Figure 5b shows the current–voltage relationships in the absence and presence of 10 μM flavoxate, and the inhibition showed a voltage-dependency (Figure 5c). This voltage-dependency was investigated before and after application of 30 μM flavoxate using the experimental protocol shown in Figure 6 (conditioning pulse duration, 8 s; holding membrane potential, −90 mV). In the absence of flavoxate (control), inactivation of the Ba^{2+} current occurred with depolarizing pulses positive to −50 mV. After application of 30 μM flavoxate (approximately 5 min later), the voltage-dependent inactivation curve in the same cells was shifted to the left (Figure 6).

As shown in Figure 7, when a depolarizing pulse was applied from a holding potential of −90 mV after an interval of 4 min in the presence of 30 μM flavoxate, the peak amplitude of the Ba^{2+} inward current was smaller (0.64 ± 0.07, $n = 5$) than that observed before application of flavoxate; however, it was consistently larger than that recorded at 4 min with repetitive application of the depolarizing pulses (0.6 ± 0.02, $n = 4$). Similar reduction of the peak amplitude of the first depolarizing pulse after 4 min application of flavoxate was observed at the different holding potential (−120 mV, 0.66 ± 0.09, $n = 5$). On removal of flavoxate, the peak amplitude of the Ba^{2+} inward current gradually recovered, but did not recover to the control level.

Immunohistochemical localization of $Ca_V1.2$ in human urinary bladder

As a search for the molecular correlate of $Ca_V1.2$ (α_{1C}, i.e., L-type Ca^{2+} currents) characterized above, immunohistochemistry was performed to detect the expression of the $Ca_V1.2$ antigen (Figure 8a, b). As shown in Figure 8b, the $Ca_V1.2$ immunoreactivity is clearly visible in the membranes of the smooth muscle cells. In contrast, no specific immunoreactive signal was seen when primary antibody was preadsorbed with the immunizing $Ca_V1.2$ antigen

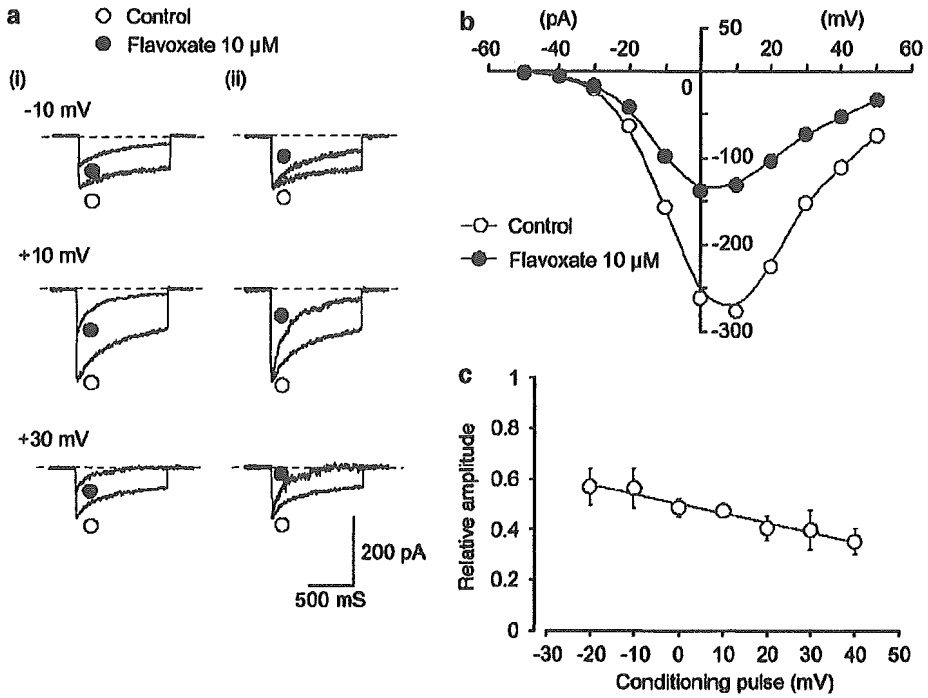

Figure 5 Effects of flavoxate on voltage-dependent Ba^{2+} inward currents at a holding membrane potential of −60 mV in human detrusor. The pipette solution was Cs^+-TEA^+ solution containing 5 mM EGTA and the bath solution was 10 mM Ba^{2+} containing 135 mM TEA^+. (a) (i) Original current traces before (control) and after application of 10 μM flavoxate at the indicated pulse potentials. (ii) Inward Ba^{2+} current from (i) scaled to match their peak amplitudes and superimposed. (b) Current–voltage relationships obtained in the absence (control) or presence of 10 μM flavoxate. The current amplitude was measured as the peak amplitude of the Ba^{2+} inward current in each condition. The lines were drawn by eye. (c) Relationship between the test potential and relative value of the Ba^{2+} inward currents inhibited by 10 μM flavoxate, expressed as a fraction of the peak amplitude of the Ba^{2+} inward current evoked by various amplitudes of depolarizing pulse in the absence of flavoxate. Each symbol indicates the mean of five observations with ± s.d. shown by vertical lines. The line was drawn by eye.

(Figure 8c, d). Immunohistochemistry using nonimmune rabbit IgG instead of primary antibody also gave a negative result (data not shown).

Discussion

The present study provides the first direct electrophysiological evidence that flavoxate, a spasmolytic agent, inhibits L-type Ca^{2+} channels in human detrusor smooth muscle.

Inhibitory potency of flavoxate in urinary bladder

Previously, Malkowicz *et al.* (1987) concluded from tension measurements that flavoxate possessed no Ca^{2+} antagonist properties in rabbit detrusor. However, it has been reported that flavoxate causes a concentration-dependent relaxation of the tension elicited by muscarinic stimulation ($IC_{50}=35\,\mu$M) or 5 mM extracellular Ca^{2+} ($IC_{50}=83\,\mu$M) in rat detrusor (Kimura *et al.*, 1996). In the present experiments, we found that flavoxate caused a concentration-dependent relaxation of human urinary bladder precontracted by K^+ with much higher potency ($IC_{50}=2\,\mu$M). It is unknown at present whether nor not the different potency of flavoxate is due to the species difference. Furthermore, in human urinary bladder myocytes, we have been able to demonstrate directly that flavoxate suppressed voltage-dependent Ba^{2+} currents through L-type Ca^{2+} channels in a concentration-dependent manner by use of patch-clamp techniques. In rabbit detrusor myocytes, flavoxate also inhibited voltage-dependent Ba^{2+} currents with a similar potency ($K_i=9\,\mu$M, unpublished observation, Teramoto). Thus, we suggest that flavoxate may possess a Ca^{2+} antagonistic action in human and rabbit detrusor myocytes and suppresses the contraction evoked by K^+.

There is a small discrepancy regarding the potency of flavoxate between tension measurements ($IC_{50}=2\,\mu$M) and patch-clamp experiments ($K_i=10\,\mu$M) in human urinary bladder. Since the K^+-induced contraction probably results both from the membrane depolarization and release of ATP and ACh from the nerve terminals in the tissues, several mechanisms in the smooth muscles may be activated, including voltage-dependent Ca^{2+} channels and receptor-operated Ca^{2+} entry pathways, etc. (reviewed by McFadzean & Gibson, 2002). It is conceivable that flavoxate may also modulate the other Ca^{2+} entry pathways, thus showing a stronger potency to inhibit the contractions than to suppress voltage-dependent Ca^{2+} currents in human detrusor.

Kinetic studies concerning the actions of flavoxate on voltage-dependent Ba^{2+} currents

The same amplitude of voltage-dependent Ba^{2+} currents was produced by application of depolarizing pulses from holding membrane potentials of −90 mV or more negative values,

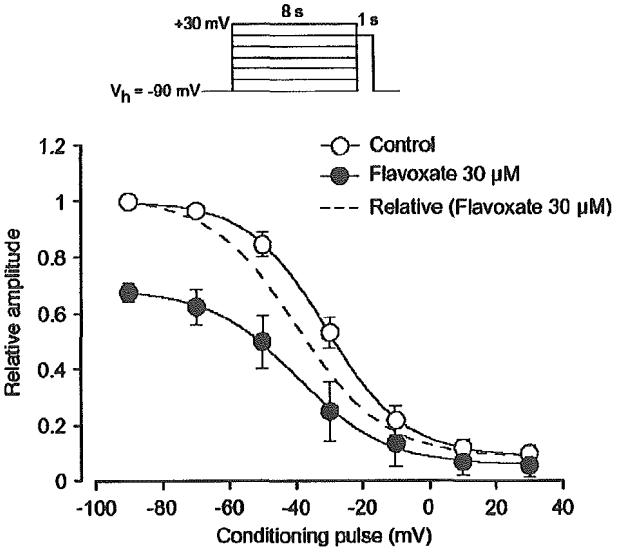

Figure 6 Effects of flavoxate (30 μM) on the voltage-dependent inactivation of the Ba^{2+} inward currents in human detrusor. Whole-cell recording, pipette solution Cs^+-TEA^+ solution containing 5 mM EGTA and bath solution 10 mM Ba^{2+} containing 135 mM TEA^+. The holding potential was −90 mV. Conditioning pulses of various amplitudes were applied (up to +30 mV, 8 s duration) before application of the test pulse (to +10 mV, 1 s duration). An interval of 20 ms was allowed between these two pulses to estimate possible contamination of the capacitive current. The peak amplitude of Ba^{2+} current evoked by each test pulse was measured before and after application of 30 μM flavoxate. The curves with the solid line; the peak amplitude of Ba^{2+} inward current in the absence and presence of flavoxate without application of any conditioning pulse was normalized as one. The curve with the broken line was normalised to the current at +10 mV upon stepping from −90 mV in 30 μM flavoxate. The lines were draw by fitting the data to the following equation in the least-squares method: $I=(I_{max}-C)/\{1+\exp[(V-V_{half})/k]\}+C$, where I, I_{max}, V, V_{half}, k and C are the relative amplitude of Ba^{2+} inward currents observed at various amplitude of the conditioning pulse (I) and observed with application of the conditioning pulse of −90 mV (I_{max}), amplitude of the conditioning pulse (V), and that where the amplitude of Ba^{2+} inward current was reduced to half (V_{half}), slope factor (k) and fraction of the noninactivating component of Ba^{2+} inward current (C). The curves in the absence or presence of flavoxate were drawn using the following values: (control), $I_{max}=1$, $V_{half}=-31$, $k=12$ and $C=0.09$ (flavoxate, 30 μM), $I_{max}=0.68$, $V_{half}=-40$, $k=13$ and $C=0.06$. Each symbol indicates the mean of 5–6 observations with ± s.d. shown by vertical lines. Some of the s.d. bars are less than the size of the symbol.

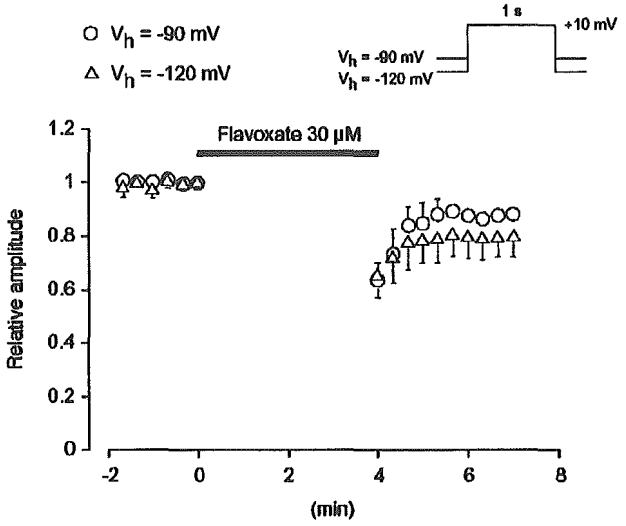

Figure 7 The effects of flavoxate on voltage-dependent Ba^{2+} currents. No pulses were applied for the initial 4 min after application of 30 μM flavoxate. Each symbol shows the size of the mean value of the peak amplitude of the voltage-dependent Ba^{2+} current evoked by the depolarizing pulses after this 4 min from two holding potentials (−90 mV, 0.64 ± 0.07, $n=5$; −120 mV, 0.66 ± 0.09, $n=5$). The peak amplitude of the voltage-dependent Ba^{2+} current just before application of flavoxate was normalized as one (control).

suggesting that all of the voltage-dependent Ca^{2+} channels at these potentials may be in the resting state. The ability of 30 μM flavoxate to suppress the peak amplitude of the Ba^{2+} currents evoked by a depolarizing pulse from two different holding potentials (−90 and −120 mV) were not significantly different, suggesting that at these negative holding potentials, flavoxate may inhibit the Ba^{2+} currents in a voltage-independent manner (resting state block). When the holding potential was elevated to −60 mV, voltage-dependent inhibition by flavoxate was observed and the concentration response curve was shifted to the left. The voltage-dependent inactivation curve was also shifted to the left after application of 30 μM flavoxate. These results suggest the voltage-dependent inhibitory actions of flavoxate occur at the inactivated state of the Ca^{2+} channels in human urinary bladder (voltage-dependent block). In the present experiments, the K_{rest} value was estimated to be 56 μM from the concentration–response curve at a holding potential of −90 mV. When ΔV_{half} value was obtained from the results using 8 s conditioning pulses, the estimated K_{inact} value was 8.6 μM (see Methods). Given this, we suggest that flavoxate may bind to the inactivated state with approximately 6.5 times higher affinity than to the resting state in human detrusor.

Pharmacological properties of flavoxate in lower urinary tract

The options for clinical treatment of urge frequency of micturition and overactive bladder (OAB) are currently behavioral techniques, pharmacological agents and surgical procedures. Owing to its availability, immediacy of results and convenience, pharmacotherapy (such as anticholinergic drugs, spasmolytic agents, estrogen) has advanced to alleviate the detrusor overactivity. Anticholinergic agents (such as oxybutynin, tolterodine and trospium chloride, etc.) are the most commonly used drugs (reviewed by Hegde *et al.*, 2004). Binding studies have revealed that flavoxate also exhibits a weak but significant anticholinergic activity on muscarinic receptors ($IC_{50}=12$ μM, Abbiati *et al.*, 1988). However, the anticholinergic activity of flavoxate was much less potent than those of other anticholinergic agents (oxybutynin, $IC_{50}=5$ nM; tolterodine, $IC_{50}=588$ nM, Abbiati *et al.*, 1988), and it is difficult to justify classification of flavoxate as an anticholinergic compound. Although efficacious as therapy for urge frequency of micturition, anticholinergic actions typically produced dry mouth, difficulty in visual accommodation, constipation and somnolence. In order to reduce these predictable side effects, much effort is currently being spent to find new approaches (such as α_1 antagonists, β_3 stimulants, K^+ channel openers, etc.) for the treatment of urge frequency

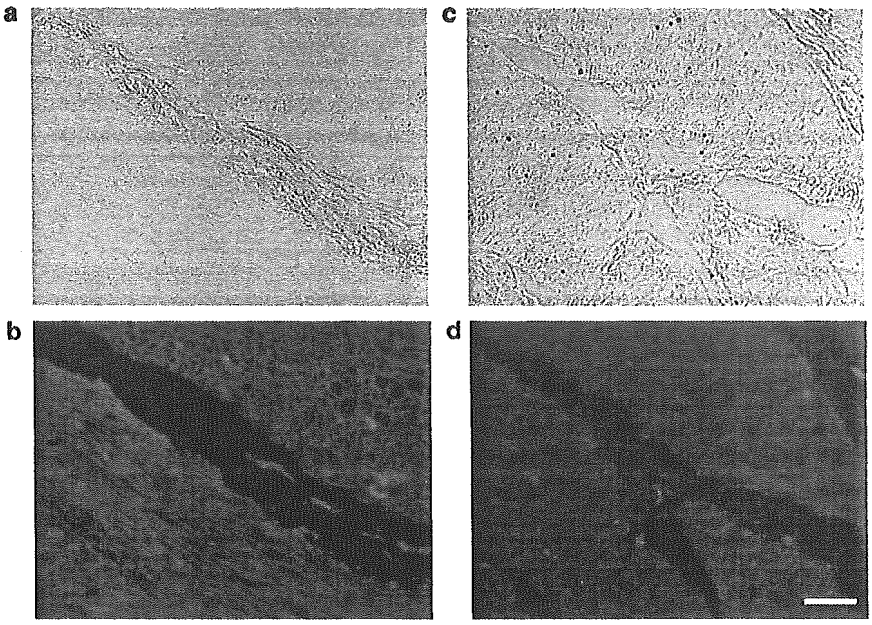

Figure 8 Fluorescent images of immunoreactivity for $Ca_V1.2$ in the human detrusor bundles. (a, b) $Ca_V1.2$ immunoactivity; clear membranous staining was observed at the tissues of the human urinary bladder smooth muscle layers. (c, d) Negative control: use of $Ca_V1.2$ antibody preadsorbed with the immunizing antigen never yields any colour reaction. Bar (white line in (d)) represents 200 μm.

of micturition and OAB (reviewed by Andersson, 2004). In the present experiments, we have been able to demonstrate that flavoxate possesses a direct Ca^{2+} antagonistic action on voltage-dependent L-type Ca^{2+} currents in human detrusor in addition to the actions as a modulator of the micturition centre in CNS (see Introduction). Thus, it seems plausible that the Ca^{2+} antagonistic actions of flavoxate are related to its spasmolytic effects on human urinary bladder. However, higher concentrations of flavoxate are required to cause the inhibitory effects on voltage-dependent L-type Ca^{2+} currents in comparison to those in CNS. Andersson (1993) queried the usefulness of Ca^{2+} antagonists for the treatment of urinary incontinence and OAB due to their poor tissue selectivity. Further studies may be still necessary to work out the full details of binding site(s) for flavoxate.

In conclusion, we have been able to demonstrate that flavoxate caused a detrusor relaxation through inhibition of L-type Ca^{2+} channel in human urinary bladder.

We thank Professor Alison F. Brading (University, Department of Pharmacology, Oxford, U.K.) for her helpful discussion and critical reading of the manuscript. This work was supported by a Grant-in-Aid for Scientific Research (B)-(2) from the Japanese Society for the Promotion of Science (Noriyoshi Teramoto, Grant Number 16390067). We thank Mr Hiroshi Fujii for his excellent help with histological experiments.

References

ABBIATI, G.A., CESERANI, R., NARDI, D., PIETRA, C. & TESTA, R. (1988). Receptor binding studies of the flavone, REC 15/2053, and other bladder spasmolytics. *Pharm. Res.*, **5**, 430–433.

ANDERSSON, K.E. (1993). Pharmacology of lower urinary tract smooth muscles and penile erectile tissues. *Pharmacol. Rev.*, **45**, 253–308.

ANDERSSON, K.E. (2004). New pharmacologic targets for the treatment of the overactive bladder: an update. *Urology*, **63**, 32–41.

HAEUSLER, G., LEITICH, H., VAN TROTSENBURG, M., KAIDER, A. & TEMPFER, C.B. (2002). Drug therapy of urinary urge incontinence: a systematic review. *Obstet. Gynecol.*, **100**, 1003–1016.

HEGDE, S.S., MAMMEN, M. & JASPER, J.R. (2004). Antimuscarinics for the treatment of overactive bladder: current options and emerging therapies. *Curr. Opin. Invest. Drugs*, **5**, 40–49.

KAJIOKA, S., NAKAYAMA, S., MCMURRAY, G., ABE, K. & BRADING, A.F. (2002). Ca^{2+} channel properties in smooth muscle cells of the urinary bladder from pig and human. *Eur. J. Pharmacol.*, **443**, 19–29.

KASEDA, M., SATO, A., SATO, Y. & TORIGATA, Y. (1975). Effects of flavoxate hydrochloride (AK-123) on the vesical functions in rats. *Clin. Physiol.*, **5**, 540–547.

KIMURA, Y., SASAKI, Y., HAMADA, K., FUKUI, H., UKAI, Y., YOSHIKUNI, Y., KIMURA, K., SUGAYA, K. & NISHIZAWA, O. (1996). Mechanisms of the suppression of the bladder activity by flavoxate. *Int. J. Urol.*, **3**, 218–227.

KOHLER, F.P. & MORALES, P.A. (1968). Cystometric evaluation of flavoxate hydrochloride in normal and neurogenic bladders. *J. Urol.*, **100**, 729–730.

MALKOWICZ, S.B., WEIN, A.J., RUGGIERI, M.R. & LEVIN, R.M. (1987). Comparison of calcium antagonist properties of antispasmotic agents. *J. Urol.*, **138**, 667–670.

MCFADZEAN, I. & GIBSON, A. (2002). The developing relationship between receptor-operated and store-operated calcium channels in smooth muscle. *Br. J. Pharmacol.*, **135**, 1–13.

OKA, M., KIMURA, Y., ITOH, Y., SASAKI, Y., TANIGUCHI, N., UKAI, Y., YOSHIKUNI, Y. & KIMURA, K. (1996). Brain pertussis toxin-sensitive G proteins are involved in the flavoxate hydrochloride-induced suppression of the micturition reflex in rats. *Brain Res.*, **727**, 91–98.

PÉRÉON, Y., DETTBARN, C., LU, Y., WESTLUND, K.N., ZHANG, J.T. & PALADE, P. (1998). Dihydropyridine receptor isoform expression in adult rat skeletal muscle. *Pflügers Arch.*, **436**, 309–314.

TERAMOTO, N. & BRADING, A.F. (1996). Activation by levcromakalim and metabolic inhibition of glibenclamide-sensitive K channels in smooth muscle cells of pig proximal urethra. *Br. J. Pharmacol.*, **118,** 635–642.

TERAMOTO, N., BRADING, A.F. & ITO, Y. (2003). Multiple effects of mefenamic acid on K^+ currents in smooth muscle cells from pig urethra. *Br. J. Pharmacol.*, **140,** 1341–1350.

TERAMOTO, N., YUNOKI, T., IKAWA, S., TAKANO, N., TANAKA, K., SEKI, N., NAITO, S. & ITO, Y. (2001). The involvement of L-type Ca^{2+} channels in the relaxant effects of the ATP-sensitive K^+ channel opener ZD6169 on pig urethral smooth muscle. *Br. J. Pharmacol.*, **134,** 1505–1515.

UCKERT, S., STIEF, C.G., ODENTHAL, K.P., TRUSS, M.C., LIETZ, B. & JONAS, U. (2000). Responses of isolated normal human detrusor muscle to various spasmolytic drugs commonly used in the treatment of the overactive bladder. *Arzneimittelforschung,* **50,** 456–460.

UEHARA, A. & HUME, J.R. (1985). Interactions of organic calcium channel antagonists with calcium channels in single frog atrial cells. *J. Gen. Physiol.*, **85,** 621–647.

YOSHIMURA, N., SASA, A., YOSHIDA, O. & TAKAORI, S. (1992). Inhibitory effects of Hachimijiogan on micturition reflex *via* locus coeruleus. *Folia Pharmacol. Jpn.*, **99,** 161–166.

(Received February 15, 2005
Revised April 1, 2005
Accepted April 20, 2005
Published online 20 June 2005)

Human Pathology (2005) 36, 330–340

ELSEVIER

Human PATHOLOGY

www.elsevier.com/locate/humpath

Angiogenesis and lymphangiogenesis and expression of lymphangiogenic factors in the atherosclerotic intima of human coronary arteries☆

Toshiaki Nakano MD[a,b], Yutaka Nakashima MD, PhD[a], Yoshikazu Yonemitsu MD, PhD, FAHA[a,*], Shinji Sumiyoshi MD[a], Young-Xiang Chen PhD[a], Yuri Akishima MD[c], Toshiharu Ishii MD, PhD[c], Mitsuo Iida MD, PhD[b], Katsuo Sueishi MD, PhD[a]

[a]*Division of Pathophysiological and Experimental Pathology, Department of Pathology, Graduate School of Medical Sciences, Kyushu University, Fukuoka 812-8582, Japan*
[b]*Department of Medicine and Clinical Science, Graduate School of Medical Sciences, Kyushu University, Fukuoka 812-8582, Japan*
[c]*Department of Pathology, School of Medicine, Toho University, Tokyo, Japan*

Keywords:
Coronary artery;
VEGF-C;
Atherosclerosis;
Angiogenesis;
Lymphangiogenesis

Summary Little information regarding the development of lymphangiogenesis in coronary atherosclerosis is available. We immunohistochemically investigated the correlation among intimal neovascularization (CD34 for angiogenesis and lymphatic vessel endothelial hyaluronan receptor-1 [LYVE-1] and podoplanin for lymphangiogenesis), the expression of lymphangiogenic factors (vascular endothelial growth factor [VEGF]-C and VEGF-D), and the progression of atherosclerosis using 169 sections of human coronary arteries from 23 autopsy cases. The more the atherosclerosis advanced, the more often the neointimas contained newly formed blood vessels ($P < .0001$). Vascular endothelial growth factor-C was expressed mostly in foamy macrophages and in some smooth muscle cells, whereas VEGF-D was abundantly expressed in both. The number of VEGF-C–expressing cells, but not that of VEGF-D–expressing cells, was increased as the lesion advanced and the number of intimal blood vessels increased ($P < .01$). Lymphatic vessels were rare in the atherosclerotic intima (LYVE-1 vs CD34 = 13 vs 3955 vessels) compared with the number seen in the adventitia (LYVE-1 vs CD34 = 360 vs 6921 vessels). The current study suggests that VEGF-C, but not VEGF-D, may contribute to plaque progression and be a regulator for angiogenesis rather than lymphangiogenesis in coronary atherosclerotic intimas. Imbalance of angiogenesis and lymphangiogenesis may be a factor contributing to sustained inflammatory reaction during human coronary atherogenesis.

☆ This work was supported in part by a Grant-in-Aid (YY and KS) from the Japanese Ministry of Education, Culture, Sports, Science, and Technology.

Abbreviations: VEGF, vascular endothelial growth factor; VEGFR, vascular endothelial growth factor receptor; AHA, American Heart Association; SMC, smooth muscle cell; LYVE-1, lymphatic vessel endothelial hyaluronan receptor-1; DIT, diffuse intimal thickening.

* Corresponding author. Division of Pathophysiological and Experimental Pathology, Department of Pathology, Graduate School of Medical Sciences, Kyushu University 3-1-1 Maidashi, Higashi-ku, Fukuoka 812-8582, Japan.

E-mail address: yonemitu@patho11.med.kyushu-u.ac.jp (Y. Yonemitsu).

0046-8177/$ – see front matter
doi:10.1016/j.humpath.2005.01.001